Laboratory of Organic Optics and Electronics

Academic and Research Staff
Professor Marc Baldo

Collaborators
Joseph Shinar[1], Zoltan Soos[2], Nikolai Lebedev[3], Barry Bruce[4], Francesco Stellacci,[5] Shuguang Zhang[6]

Graduate Students
Rupa Das, Michael Segal, Patrick J. Kiley, Julie Norville, Rajay Kumar, Benjie Limketkai

Support Staff
Jacques Wood

Introduction
Molecular electronics is one of a number of competing approaches to the problem of employing nanotechnology to increase the performance of electronic devices. Molecules possess some potential advantages for nanoelectronics: chemistry offers a unique ability to tailor features at the nanoscale, molecules may be semiconducting, they can de designed to assemble on specific sites in a circuit, and they possess unique properties such as mechanical flexibility that may enable novel devices such as electromechanical switches. But molecular electronics is in its infancy, hampered by a lack of theoretical understanding, and also the fabrication challenge of building and testing molecular scale devices. This work examines various aspects of molecular physics and technology: from prototypical molecular electronic circuits (photosynthetic complexes), to charge transport at metal-molecule interfaces.

Much of the work is necessarily interdisciplinary, and has involved important collaborations with biologists, notably, Prof. Barry Bruce at the University of Tennessee, Knoxville, and Dr Nikolai Lebedev at the U.S. Naval Research Laboratory. Studies of excitons were performed with Prof. Zoltan Soos in the Department of Chemistry at Princeton University, and also the spectroscopy group of Prof. Joseph Shinar at Iowa State University.

1. Fundamental Efficiency Limits of Electroluminescence in Organic Semiconductors

Sponsors
National Science Foundation MRSEC, Universal Display Corporation

Project Staff
Michael Segal, Professor Marc Baldo

The electronic and luminescent behavior of organic semiconductors is determined in large part by the properties of excitons. These are neutral excitations that participate in radiative processes and transport energy within a film. Perhaps their most fundamental property is spin, which determines their lifetime, energy, physical size, and their ability to radiatively decay. Yet the crucial processes that determine the spin of an exciton remain obscure.

[1] Ames Laboratory and Physics and Astronomy Department, Iowa State University
[2] Department of Chemistry, Princeton University
[3] Center for Bio/Molecular Science and Engineering, U.S. Naval Research Laboratory
[4] Department of Biochemistry, Cellular and Molecular Biology, University of Tennessee
[5] Department of Materials Science and Engineering, MIT
[6] Center for Biomedical Engineering, MIT

This project seeks to understand and explain the spin selection process in excitons of molecules and polymers, thereby illuminating the exciton creation process. In the simplest model, excitons created from charge injection should be divided according to spin-degeneracy into $\chi = 25\%$ singlets (total spin, $S = 0$) and 75% triplets ($S = 1$). But evidence exists suggesting that conjugation length may affect the ultimate ratio of singlets to triplets.[1-7] Several studies have suggested that the singlet fraction in conjugated polymeric materials may be considerably higher than $\chi = 25\%$,[1,3-7] while the singlet fraction in small molecular weight materials appears to be somewhat lower than $\chi = 25\%$.[2,5]

In addition to the physics that may be revealed, quantification of the ratio of singlet to triplet excitons is critical to organic electroluminescent technology. By harnessing triplets and singlets, phosphorescent organic light emitting devices (OLEDs) exhibit efficiencies approximately four times that of molecular OLEDs that fluoresce from singlets alone; see Fig. 1.[8] But if $\chi > 25\%$ in polymers then fluorescent polymers may possess intrinsically higher electroluminescent efficiencies than fluorescent small molecules.

We have developed a novel technique for determining the fraction, χ, of luminescent singlet excitons in an organic semiconductor. Critical to the measurement is an accurate determination of the photoluminescent (PL) efficiency of an organic semiconductor. In PL, an optical pump generates only singlet excitons. In this project, we measure PL efficiency by optically exciting the luminescent organic film under reverse electrical bias. The electric field dissociates some excitons into charges, reducing the PL and generating photocurrent, thereby providing an accurate measurement of the number of excitons dissociated. This technique is convenient because the electroluminescent (EL) efficiency may be measured in the same experimental geometry by applying forward bias to the luminescent film and injecting charges.

The experimental setup for the measurement is shown in Fig. 2. Typical characteristics for the reverse bias photocurrent, I_{ph}, and the field-induced change in PL, ΔP_{PL}, are shown in Fig. 3 for the archetypal polymer poly[2-methoxy-5-(2-ethylhexyloxy)-1,4-phenylenevinylene] (MEH-PPV). A weighted sum of several measurements yields $\eta_C \eta_{PL} = (2.1 \pm 0.3)\%$ for MEH-PPV. When compared to the EL efficiencies of the same devices we get $\chi = (21 \pm 5)\%$ for MEH-PPV, inconsistent with models that predict $\chi > 25\%$. The results demonstrate that polymeric materials possess no intrinsic advantage in fluorescent efficiency compared to small-molecular weight materials.

Magnetic resonance provides another essential tool for studying the spin dependence of exciton formation. However, the interpretation of optically-detected magnetic resonances (ODMR) in π-conjugated polymers remains controversial. We have studied the frequency dependence of a photoluminescence-detected resonance when both the optical excitation and the microwave energy are modulated. In contrast to the frequency dependence of the microwave modulation, the double modulated signal is flat between 1 kHz and 100 kHz, confirming the significance of singlet exciton quenching to the resonance. We propose that the spin-dependent behavior in the resonance is explained by triplet-polaron interactions; see Fig. 4.

References

1. Y. Cao, I. Parker, G. Yu, Z. C, and A. Heeger, Nature 397: 414 (1999).
2. M. A. Baldo, D. F. O'Brien, M. E. Thompson, and S. R. Forrest, Phys. Rev. B 60: 14422 (1999).
3. J.-S. Kim, P. K. H. Ho, N. C. Greenham, and R. H. Friend, J. Appl. Phys. 88: 1073 (2000).
4. M. Wohlgenannt, K. Tandon, S. Mazumdar, S. Ramasesha, and Z. V. Vardeny, Nature 409: 494 (2001).
5. J. S. Wilson, A. S. Dhoot, A. J. A. B. Seeley, M. S. Khan, A. Köhler, and R. H. Friend, Nature 413: 828 (2001).
6. M. Wohlgenannt and Z. V. Vardeny, Synth. Met. 125: 55 (2002).
7. M. Wohlgenannt, X. M. Jiang, Z. V. Vardeny, and R. A. J. Janssen, Phys. Rev. Lett. 88: 197401 (2002).
8. M. A. Baldo, D. F. O'Brien, Y. You, *et al.*, Nature 395: 151 (1998).

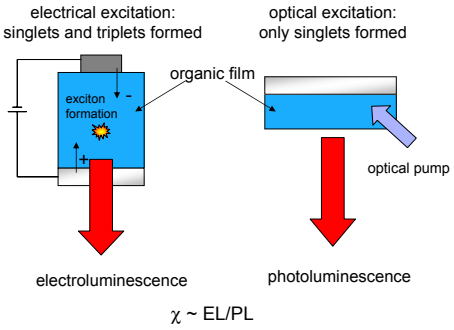

Figure 1: *Phosphorescent dopants can be used to sense triplets. Comparing fluorescence and phosphorescence then gives the singlet fraction.*

Figure 2: *The experimental setup of the reverse bias measurement: The out-coupled PL efficiency is obtained by comparing the change in PL to the photocurrent.* ***Inset.*** *A cross section of the OLEDs: charges and excitons within the organic layer under test are confined by a heterostructure employing bathocuproine (BCP) as the electron transport layer (ETL). The semiconducting polymer, MEH-PPV was used as a hole transport layer (HTL).*

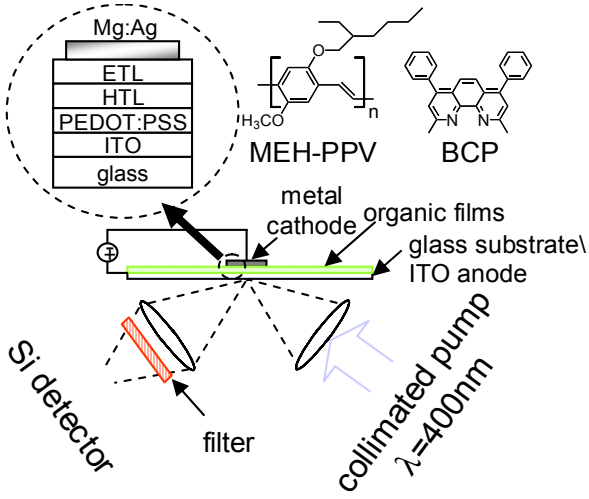

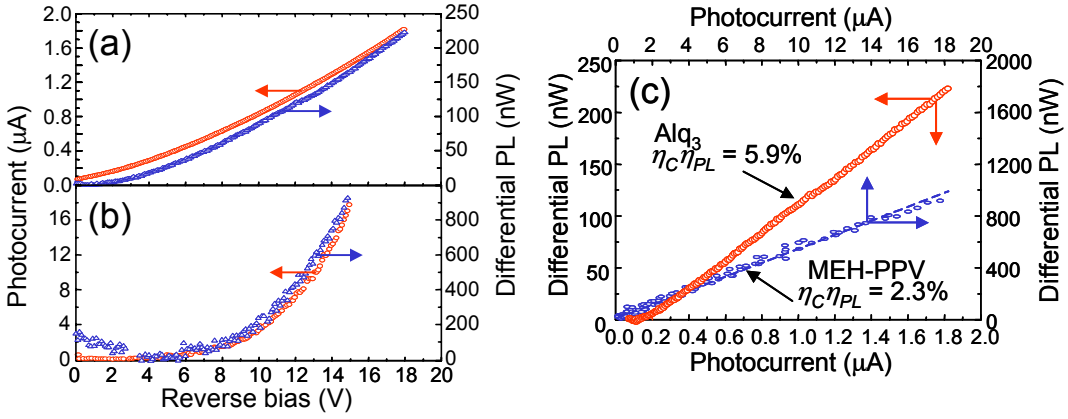

Figure 3: *The change in photoluminescence (ΔP_{PL}) and the corresponding increase in photocurrent, I_{ph}, in* ***(a)*** *Alq_3 and* ***(b)*** *MEH-PPV, respectively, as a function of reverse bias.* ***(c)*** *The relation between ΔP_{PL} and I_{ph} gives the out-coupled PL efficiency, $\eta_C \eta_{PL}$.*

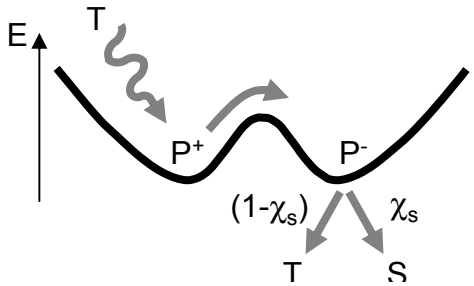

Figure 4: *In the triplet-polaron model of magnetic resonances in organic semiconductors, triplet excitons, T, collide with trapped polaron pairs, initiating recombination, and reducing the population of quenching species in the film. This increases the photoluminescent efficiency of the film.*

2. Solid State Integration Of Photosynthetic Protein Molecular Complexes

Sponsors
DARPA/AFOSR F49620-02-1-0399, National Science Foundation MRSEC

Project Staff
Rupa Das, Patrick J. Kiley, Michael Segal, Julie Norville, Rajay Kumar, Professor Marc Baldo

Over two billion years of evolutionary adaptation have optimized the functionality of biological photosynthetic complexes. Plants and photosynthetic bacteria, for example, contain protein molecular complexes that harvest photons with nearly optimum quantum yield and an expected power conversion efficiency exceeding 20%.

The molecular circuitry within photosynthetic complexes is organized by a protein scaffold. At present, conventional technology cannot equal the density of the molecular circuitry found in photosynthetic complexes. But if integrated with solid state electronics, photosynthetic complexes might offer an attractive architecture for future generations of circuitry where molecular components are organized by a macromolecular scaffold.

We have demonstrated the solid state integration of photosynthetic complexes. The functionality of the complexes is tested by fabricating solid state photodetectors and photovoltaic devices, using complexes isolated from spinach leaves or photosynthetic bacteria. The internal quantum efficiency of the first generation of devices is estimated to be 12%. The major application of photosynthetic photovoltaics is intended to be solar cells for weight-critical applications such as micro aerial vehicles (MAVs).

Stabilizing the complexes in an artificial environment is the key barrier to successful device integration. We achieved electronic integration of devices (see Fig. 1) by stabilizing an oriented, self-assembled monolayer of photosynthetic complexes using novel surfactant peptides, (see Fig. 2) and then depositing an organic semiconducting protective coating, required as a buffer to prevent damage to the complexes when depositing the top metal contact.

Successful integration is conclusively demonstrated by comparisons of the absorption spectrum and photocurrent spectra in Fig. 3 (inset) and Fig. 4. Further work will harness the full (up to 1.1V) open circuit voltage of complexes such as Photosystem I, and enhance the optical cross section of these devices.

Solid-state integration of biological photosynthetic complexes

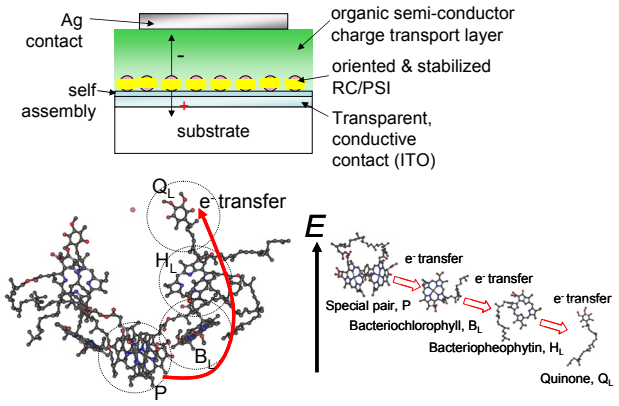

Figure 1: ***(top left)*** *The structure of solid-state devices incorporating photosynthetic complexes.* ***(bottom left)*** *The internal molecular circuitry of a photosynthetic bacterial reaction center with the protein scaffold removed for clarity. The complex is only a few nanometers top-to-bottom. After photoexcitation, an electron is transferred from the special pair, P, to the quinone, Q_L. The process occurs within 200ps, at nearly 100% quantum efficiency, and results in a 0.5V potential across the complex.*

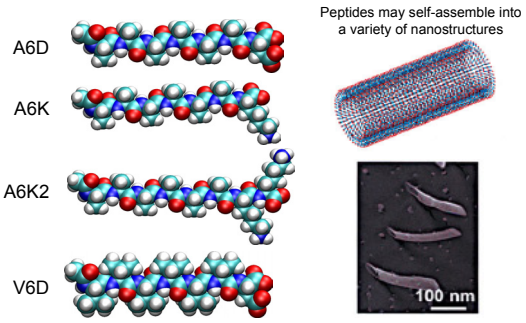

Figure 2: *Stabilization during and after fabrication is the key to successful solid-state integration of biological molecular circuits. A selection of novel peptides, previously demonstrated to self-assemble in nanorods and nanovesicles. These enabled stabilization and solid-state device integration.*

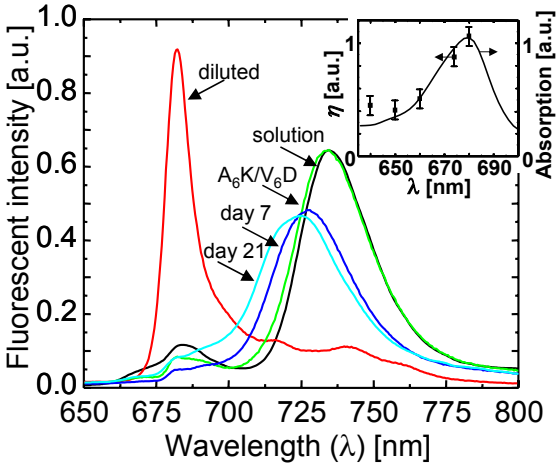

Figure 3: *A comparison between the fluorescence spectrum of a frozen (T = 10K) solution of photosynthetic complexes (in this case Photosystem I – PSI) as extracted from spinach, with washed and dried films of PSI demonstrates that this complex may be protected against degradation after washing and drying steps by stabilizing with the surfactant peptides A_6K and V_6D. The stabilizing action of A_6K/V_6D is preserved for several weeks for dried films left in ambient conditions.* ***Inset:*** *the stabilized PSI devices exhibit a photocurrent spectrum that matches the absorption spectrum, confirming solid state integration of stabilized PSI.*

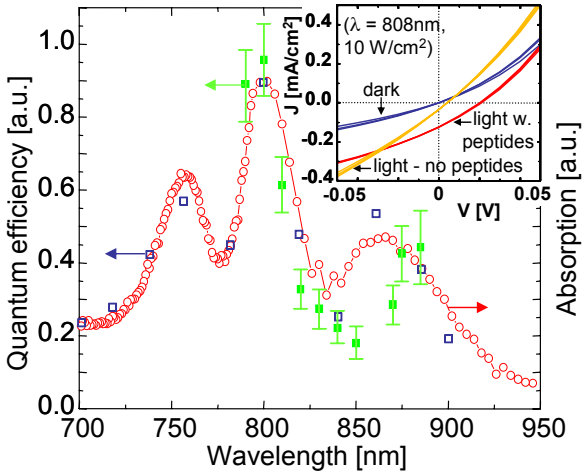

Figure 4: *The photocurrent spectrum of solid-state photovoltaic devices employing bacterial reaction centers (RCs). A comparison between the photocurrent spectrum of solid-state (■) and wet electrochemical cell devices (Y), and the solution absorption spectrum of the bacterial reaction centers (–o–), demonstrates that the observed photocurrent originates in the RCs.* ***Inset****: stabilization of RC complexes with A_6K/V_6D peptides improves the internal quantum efficiency of the devices to 12% under short circuit conditions.*

3. The Effect of Disorder on Electron Injection into Organic Semiconductors

Sponsor
MARCO Materials Structures and Devices Center

Project Staff
Benjie Limketkai, Professor Marc Baldo

The temperature and electric-field dependence of charge injection from metals into amorphous films of organic semiconductors is a significant problem in disordered materials that has, to date, resisted description by analytic theories.[1] In this project, we have examined electron injection at interfaces between a metal cathode and an amorphous film of an organic semiconductor. It was determined that the charge transport characteristics of most electron-injecting contacts are described by a master equation valid for all cathode-doped interfaces. As a consequence we are able to explain the temperature and electric field dependence of electron injection from various metallic cathodes into organic semiconductors by varying the density of extrinsic electron donors in the organic semiconductor.

Typically, the metal-organic semiconductor interface is heavily-doped by charge transfer from the cathode. At equilibrium, the interface is partly depleted, shifting the vacuum energy by approximately 1eV. Energetic disorder significantly broadens the density of states in the depletion region and this disorder controls the charge injection process; see Fig. 1. We describe the geometry of the interface with a self-affine model,[2,3] and calculate the energetic variance in the depletion region as:

$$\sigma_I^2 = \frac{q}{2\pi}\left(\frac{qN_D w\xi z_D}{\varepsilon}\right)^2 \int_{0\le k\le k_C} \frac{\left|\sinh\left(k\left(z-z_D\right)\right)\right|^2}{\left(1+k^2\xi^2/2\alpha\right)^{1+\alpha}\left|\sinh\left(kz_D\right)\right|^2}dk \qquad (1)$$

where, w is the rms roughness, ξ is the correlation length, N_D is the doping density, $z_D = \sqrt{-2\varepsilon\Delta/qN_D}$ is the mean depletion width with built-in potential, Δ, $k_C = \pi/a_0$ is the upper cutoff frequency for intermolecular separation, a_0, and α is the roughness exponent.

The current density is then determined by the rate of charge hopping from the boundary to adjacent sites in the intrinsic layer.[4] Using the Marcus expression for charge hopping between Gaussian distributions gives a master equation:

$$J = J_0 \left(V + \Delta V\right)^m \Big/ V_0^{\,m} \tag{2}$$

where ΔV is the doping-dependent voltage shift, and m, J_0 and V_0 are constants. ΔV contains the entire cathode dependence of injection; it is equivalent to the additional voltage required to inject an amount of charge equal to the doped charge present in the boundary layer. It is shown that ΔV is proportional to the doping density and the diffusion coefficient, D, *i.e.* $\Delta V \propto D \propto \exp\left[-\lambda/4kT\right]$, where λ is the molecular reorganization energy from Marcus theory.

As shown in Fig. 2, the current-voltage characteristics of Al/LiF/Alq_3, Mg:Ag/Alq_3, Al/Alq_3, Ag/Alq_3, Al/LiF/BCP, Mg:Ag/BCP and Ag/BCP devices are all described by the master equation and are related by a temperature-dependent rigid shift in voltage, ΔV, plotted in Fig. 3. The magnitude of ΔV is determined by the doping fraction, and the temperature dependence is fit by the expected temperature dependence of the diffusion coefficient. The characteristics of Au/Alq_3, Al/BCP and Au/BCP devices, shown in the inset of Fig. 2, exhibit much higher operating voltages, and cannot be related to the other devices by a rigid shift in voltage. Consequently, Au/Alq_3, Al/BCP and Au/BCP are interpreted as undoped injection interfaces beyond the scope of the theory.

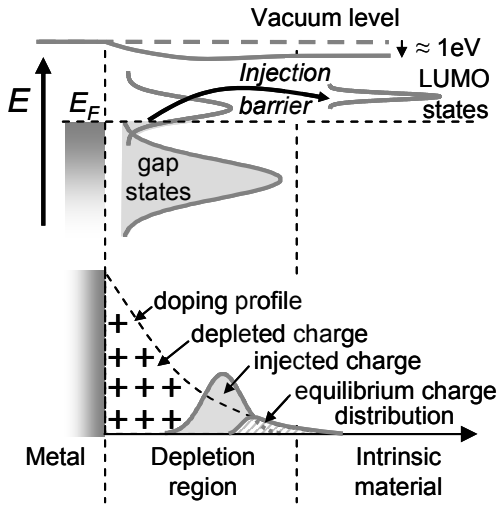

Figure 1: ***(a)*** *Based on spectroscopic studies, this is a model of the interface between a metal contact and a doped, disordered organic semiconductor. Interactions with the metal form filled gap states in the interfacial layers of the organic semiconductor. This doped charge is partially depleted at equilibrium, shifting the vacuum level at the interface. Large permanent dipole moments associated with metal dopants broaden the density of LUMO states in the interfacial region. Injection current is limited by charges hopping from the broad DOS in the interfacial region to the much narrower DOS typical of the bulk.* ***(b)*** *Doping profile of the interfacial region. The first few monolayers are depleted. Injected charge that tunnels through the depletion region is trapped in a boundary layer within the interfacial region. The presence of doped charge at the boundary reduces the operating voltage.*

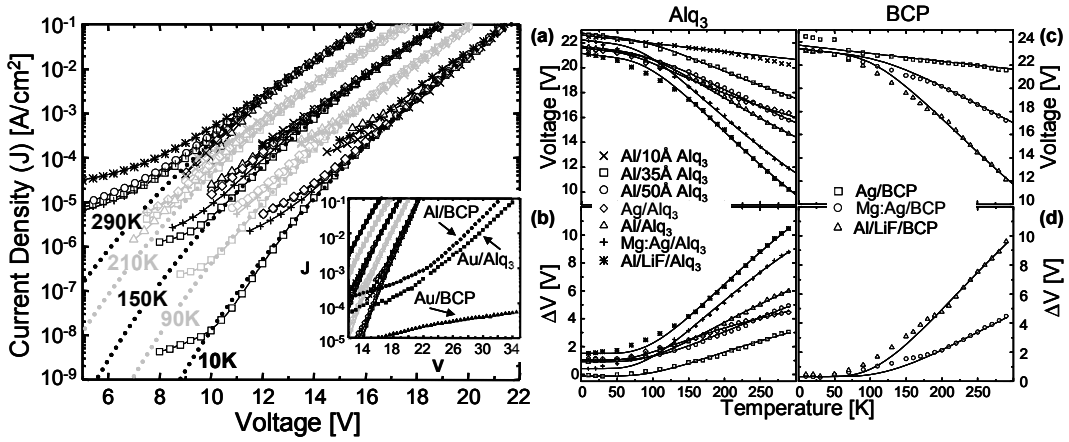

Figure 2: ***(left)*** *The temperature dependence of the IV characteristics (points) of Ag/Alq_3 (ϒ), Al/Alq_3 (○), Mg:Ag/Alq_3 (◊), Al/LiF/Alq_3 (Δ), Mg:Ag/BCP (+), Al/LiF/BCP (×), and Ag/BCP (*). The fit for $\Delta V = 0$ (fit to Al/Alq_3(10Å)/BCP) is plotted (dotted lines). A rigid voltage shift (plotted in Fig. 3b and 3d) was applied to each characteristic to overlap with the Ag/Alq_3 data.* ***Inset:*** *The IV characteristics of Au/Alq_3 (■), Al/BCP(●), and Au/BCP (▲) at room temperature cannot be made to fit the theory for doped interfaces.* **Figure 3*: (right)*** *The temperature dependence of the operating voltage at J = 1 mA/cm² for (a) doped Alq_3 interfaces, (c) doped BCP interfaces. Deviations in voltage (ΔV) from the $\Delta V = 0$ fits (Al/Alq_3(10Å)/BCP for Alq_3 and Ag/BCP for BCP) for (b) Alq_3 and (d) BCP.*

References

1. J. C. Scott, J. Vac. Sci. Technol. A 21: 521 (2003).
2. G. Palasantzas, Phys. Rev. B 48: 14472 (1993).
3. G. Palasantzas, Phys. Rev. B 49: 5785 (1994).
4. M. A. Baldo and S. R. Forrest, Phys. Rev. B 64: 085201 (2001).

Journal Articles, Published

Rupa Das, Patrick J. Kiley, Michael Segal, Julie Norville, A. Amy Yu, Leyu Wang, Scott Trammell, L. Evan Reddick, Rajay Kumar, Francesco Stellacci, Nikolai Lebedev, Joel Schnur, Barry D. Bruce, Shuguang Zhang, Marc Baldo, "Integration of Photosynthetic Protein Molecular Complexes in Solid-State Electronic Devices," *Nano Letters*, forthcoming.

Marc Baldo, Michael Segal, "Phosphorescence as a probe of exciton formation and energy transfer in organic light emitting diodes," *Phys. Stat. Sol.* 201 (6): 1205-1214 (2004)

M. Segal, M.A. Baldo, R.J. Holmes, S.R. Forrest, Z.G. Soos, "Excitonic singlet-triplet ratios in molecular and polymeric organic materials," *Physical Review B* 68: 075211 (2003)

M. Segal, M.A. Baldo, "Reverse bias measurements of the photoluminescent efficiency of semiconducting organic thin films," *Organic Electronics* 4: 191-197 (2003)